

See discussions, stats, and author profiles for this publication at: <https://www.researchgate.net/publication/339258341>

Hydrodynamic Characteristic Studies of Underwater ROV. ANSYS – Fluent Simulation

Conference Paper · October 2019

DOI: 10.1109/SIITME47687.2019.8990682

CITATION

1

READS

426

3 authors, including:



Mihaela Hnatiuc

Maritime University of Constanta

62 PUBLICATIONS 178 CITATIONS

[SEE PROFILE](#)



Khaled Chetehouna

Institut National des Sciences Appliquées Centre Val de Loire

83 PUBLICATIONS 468 CITATIONS

[SEE PROFILE](#)

Some of the authors of this publication are also working on these related projects:



underwater system [View project](#)



Fire behavior of composite materials for aeronautical applications : Experiments and Modeling [View project](#)

Hydrodynamic Characteristic Studies of Underwater ROV. ANSYS – Fluent Simulation

M. Hnatiuc¹⁾, A. Sabau¹⁾

¹⁾Maritime University Constanta
Constanta, Romania
mihaela.hnatiuc@cmu-edu.eu

K. Chetehouna²⁾

²⁾ INSA Centre Val de Loire
Bourges, France

Abstract— *This paper presents the hydrodynamic characteristic of remotely operated underwater vehicle (AUV). Using a AUV model achieved in laboratory of Constanta Maritime University, we study the hydrodynamics of the submarine using simulation to observe the floatability and the motors position. We consider the four forces on the ROV: their own weight, the Archimedes' force, the propulsion of motors and the traction force. Using some simulation, we link the traction force with the speed considering the main direction. According to the fundamental principle of statics, to maintain a constant speed, such as speed maximum, all forces must mutually cancel each other. So by designing according to each vector of the landmark. This paper is focused on how ANSYS-Fluent can point out design problems at the virtual prototype.*

Keywords— *underwater speed, hydrodynamics, floating force*

I. INTRODUCTION

This paper presents the movement control of a remotely operated underwater vehicle (Remotely Operated Vehicle - ROV). As a result of improving the manufacturing process of microcontrollers, sensors and the 3D printing process, the cost of an ROV is becoming more accessible [1]. They are used in a wide range of activities, ranging from small hobby ROVs, used for entertainment to industrial deep sea ROVs.

The common problem with most ROVs is that, most of these activities are based on the manual control of a trained operator. Thus, the efficiency of an ROV, depends to some extent on the "operator's skill", thus adding to the technical limitations and errors or limitations due to the human factor. Many of the companies that produce ROVs for industrial use, have begun to implement "depth control", where the desired depth can be automatically maintained, simplifying the task of the operators. This concept can be taken further, allowing both stationing and blocking of one or more degrees of freedom, thus maximizing the accuracy and efficiency of the ROV, at the same time reducing the time required and the complexity of operator training. These results would automatically reduce the cost of performing of operation with such an underwater robot and increase their efficiency.

ROVs are classified into categories based on size, weight, ability, power or destination [2,3]. Only the most common forms of classification will be addressed below.

Depending on the destination, they can be classified as follows:

- Military ROV
- Scientific ROV
- Educational.
- Commercial ROV.

Because commercial-type ROVs are so diverse, they can be further sub-classified into five classes:

- Class I - Observation ROV

They are usually small in size and only have a video camera or sonar. Although sometimes they can be equipped with an additional sensor, they are intended exclusively for observing the environment.

- Class II - Observation ROV with payload

They are equipped with 2 video cameras / sonar and can be equipped with several additional sensors and / or two manipulators.

- Class III - Utility ROV

This class consists of large ROVs that can be equipped with multiple manipulators or other tools and sensors.

- Class IV - towed or bottom ROV

The towed ROV moves because it is pulled by a surface craft or a winch by a cable;

The bottom ROV travels to the bottom of the ocean using a locomotion system such as wheels or tracks;

- Class V - ROV prototype

This class has the ROVs in the prototype stage or the ROVs with special destinations, which cannot be classified in the other classes.

The ROV described in this paper belongs to the education class. The system is composed by electronic components and mechanical components. The most part of electronic components is provided of BlueRobotic [4].

In the bloc diagram (Fig.1) are presented the ROV comand and control system achieved by Pixhawk and Raberry PI3. The motors are controlled by ESC (Electronic Speed Controller) and T100 propelle. The user control system is achieved by computer interface and controller. The power supply is provided by system of the accumulators and analog converter (AC and AC/DC converter). The underwater images are acquired using a camera. A pressure sensor Bar30 gives the information about the water depth and temperature.

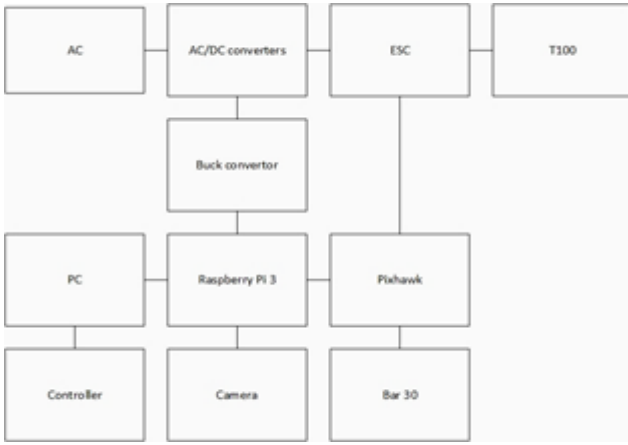


Fig.1. The electronic bloc diagramme of ROV [4]

II. SYSTEM DESCRIPTION

A. ROV movement

The ROV locomotion is provided by the thrusters, it is taken care of in terms of defining a combination of electric and propeller motors. In the design of the propulsion system, the characteristics of the propellers, such as the diameter and pitch, but also of the engine as they can be consumed and coupled, must be taken into account (Fig.2).

Another very important aspect is an engine control module. A common solution for most electric motors is required for ESC (Electronic Speed Controller). The ESC is an electronic liability circuit with the speed adjustment and distribution direction of an electric motor, which can be used automatically or dynamically.

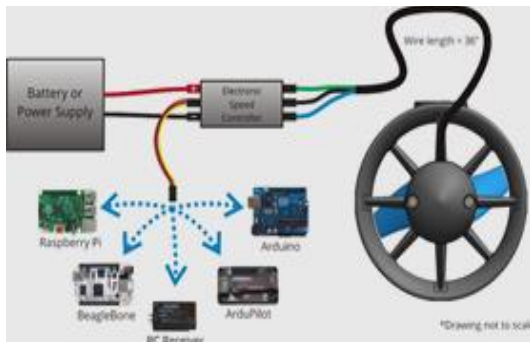


Fig. 2. ESC coupling scheme with the propulsion engine and the control microcontroller [4]

The displacement of ROV is achieved with six motors and propellers (Fig3). The propulsion motor used in the project is a DC motor without 3-phase collector brushes. This engine is controlled by the uni ESC (Electronic Speed Controller) which takes the command from the Pixhawk and transforms it into a signal specific to the T100 propulsion engine. The ESC (Electronic Speed Controller) module that is used to power the T100 propulsion engine and speed control acts as an interface module with the Pixhawk module.

The motor control use a signal as in servo motors which is time dependent. This module requires a digital signal with the filling factor 50% once at $1500 \mu s \pm 25 \mu s$. For clockwise rotation, an

impulse greater than $1500 \mu s$ in time up to $1900 \mu s$ is required which represents the maximum speed and is not recommended to be used for more than one minute. The decrease time interval of reverse rotation of the propeller is from $1500 \mu s$ to $1100 \mu s$ without exceeding one minute.



Fig.3. The electronic part of the underwater ROV

B. Comand and communication

The underwater vehicle control is a Pixhawk main control unit based on a microcontroller from ST Microelectronics. It has a Cortex-M4F processor where F at the end represents that it has a unit of 32-bit float values calculation that accelerates the computing speed but also the accuracy of the system. In addition to the base processor, the Pixhawk module has also an emergency processor that takes control the system for further use. The Pixhawk module includes a stabilization ROV system using the accelerometer, gyroscope and internal magnetometer.

The video camera is connected to the Rasbery PI3 which use Linux as operation system. If communication is done via USB from Pixhawk then no special setting is required but if using Ethernet then the network cards need to be set up. The computer that receives the data from the Raspberry Pi 3 and sends back the control commands the IP address must be 192.168.2.1 and the subnet mask 255.255.255.0.

Computer configuration starts from the control panel where we enter the networks and then we choose to change the network board settings. The user interface used in this project is QGround control. The control is performed with a Xbox 360 Logitech controller.

III. THE ROV BODY DESCRIPTION

The size of the ROV body's dimensions has been fully designed in the laboratory. Simulations in ANSYS - Fluent and SolidWork represent the design to the physical body.

A. The body type

ROV vehicles, regardless of the sensors and effectors with which they are provided, are built in two main types of architectures:

- type 1- Architecture in open frame,
- type 2-Architecture in closed hydrodynamic body

From a functional point of view, the two technical types of organization are identical.

B. The ROV body result

The chosen version combines the open frame model and the hydrodynamic body. Attempts have been made to combine

models so that the model can be used to benefit from more advantages. The most used as architecture resembles with type 2 presented above but it has elements of first type (Fig4.a). In the use phase, the ROV is the subject to four major forces: its weight, the Archimedes' thrust, the propulsion of engines, and drag force (Fig.4.b).

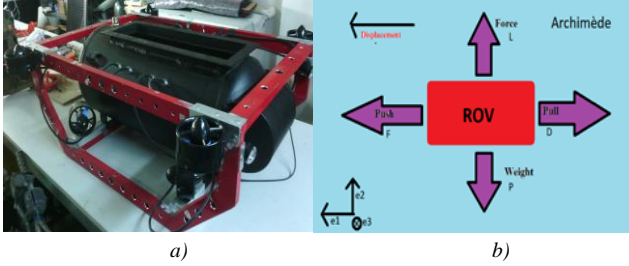


Fig.4. The underwater ROV body a) and the forces on the ROV body b)

In order to be able to do the simulation, the ROV model is modeled in Solid Works, the structure has one float (Fig. 5).

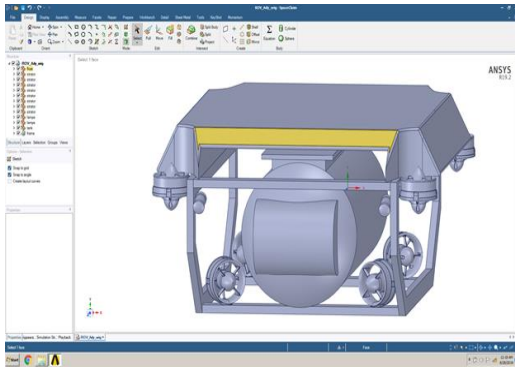


Fig.5. ROV 3D model

For the study the body is considered totally immersed and in balance. The ROV floats, thanks to the float, between the waters and moves at a constant speed. In these conditions the weight force and the Archimedeian force balance each other and the metacentric height is achieved sufficiently high to allow a stable float. These hypotheses (Fig.4b) impose the conditions presented in (1).

$$\begin{cases} P = L \\ F = D \end{cases} \quad (1)$$

The calculation field is considered paralipipedic and it's dimensions are chosen so that in any direction its size should be at least 10 times larger than that of the model. The simulation is performed on a 1:1 scale model being made in Solid Works and imported into Ansys Space Claim. The mathematical model included the Reynolds-mediated Navie-Stoks flow equations and the standard k- ε turbulence model, [5] in incompressible, stationary and isothermal regime (formula 2÷6).

The continuity formula is:

$$\frac{\partial u_i}{\partial x_i} = 0 \quad i=1,2,3 \quad (2)$$

The moment equation is:

$$\begin{aligned} \frac{\partial}{\partial t}(\rho \langle u_i \rangle) + \frac{\partial}{\partial x_j}(\rho \langle u_i \rangle \langle u_j \rangle) &= -\frac{\partial \langle p \rangle}{\partial x_i} + \\ \frac{\partial}{\partial x_j}(\langle \tau_{ij} \rangle - \rho \langle u'_i u'_j \rangle), \quad i, j &= 1, 2, 3 \end{aligned} \quad (3)$$

where:

$$\langle \tau_{ij} \rangle = \mu \left[\left(\frac{\partial \langle u_i \rangle}{\partial x_j} + \frac{\partial \langle u_j \rangle}{\partial x_i} \right) - \frac{2}{3} \frac{\partial \langle u_k \rangle}{\partial x_k} \delta_{ij} \right], \quad i, j, k=1, 2, 3 \quad (4)$$

The equations of standard k- ε turbulence model are:

$$\begin{aligned} \frac{\partial}{\partial t}(\rho k) + \frac{\partial}{\partial x_i}(\rho k u_i) &= \frac{\partial}{\partial x_j} \left[\left(\mu + \frac{\mu_t}{\sigma_k} \right) \frac{\partial k}{\partial x_j} \right] + \\ G_k + G_b - \rho \varepsilon - Y_k + S_k \end{aligned} \quad (5)$$

$$\begin{aligned} \frac{\partial}{\partial t}(\rho \varepsilon) + \frac{\partial}{\partial x_i}(\rho \varepsilon u_i) &= \frac{\partial}{\partial x_j} \left[\left(\mu + \frac{\mu_t}{\sigma_\varepsilon} \right) \frac{\partial \varepsilon}{\partial x_j} \right] + \\ C_{1\varepsilon} \frac{\varepsilon}{k} (G_k + C_{3\varepsilon} G_b) - C_{2\varepsilon} \rho \frac{\varepsilon^2}{k} + S_\varepsilon \end{aligned} \quad (6)$$

In these above formula, ρ , u_i , p , τ_{ij} represents the average values of density, velocity of pressure and stress considering their fluctuations. G_k represents the generation of turbulence kinetic energy due to the mean velocity gradients, G_b is the generation of turbulence kinetic energy due to buoyancy, Y_k represents the contribution of the fluctuating dilatation in compressible turbulence to the overall dissipation rate, and $C_{1\varepsilon}$, $C_{2\varepsilon}$, $C_{3\varepsilon}$ are constants, σ_k , σ_ε are the turbulent Prandtl numbers for k and ε , respectively. S_k , S_ε are user-defined source terms. The boundary conditions imposed are without sliding to the wall and the current velocity on the study direction (the calculation is done in the inverted system the fluid of movement with a given speed and the model is at rest (Fig.6).

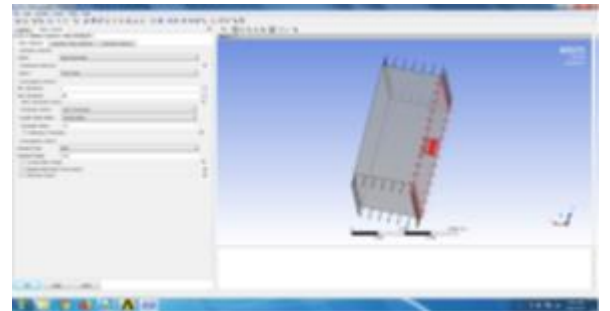


Fig.6. Boundary conditions

The system is considered in a thermodynamic balance. To reduce the computing effort, the flow is studied using the symmetry on two axes of the model. The discretization network is automatically generated using the default settings (Fig. 7).

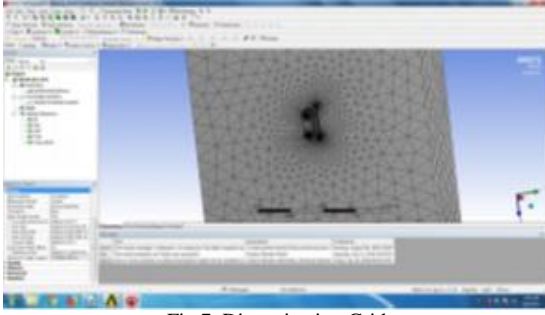


Fig.7. Discretization Grid

The simulation results aimed to obtain the velocity field and the force of the resistance to advancement on the flow direction which is proportional to the velocity square (Fig. 8).

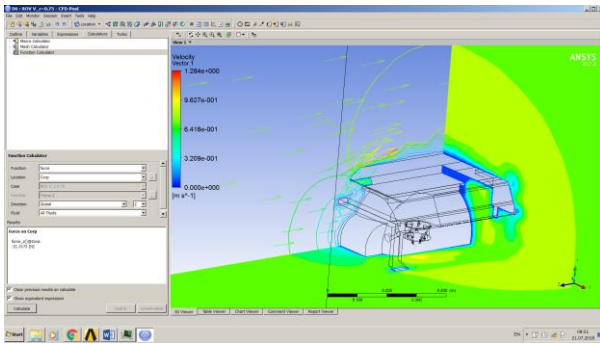


Fig.8 Velocity distribution

The results obtained from the simulations for different speeds for both forward and backward travel are presented in Table I.

TABLE 1. STRENGTH OF RESISTANCE TO ADVANCEMENT

V_z [m/s]	F_z [N]	F_z [N]
0,1	0,786	0,812
0,25	4,8	4,976
0,5	19,04	19,70
0,75	42,64	44,10
1	75,52	87,27
2	301,82	332,31

Using the interpolation data of Table I, the function $F_z(V_z)$ is obtained. This is used to determine the moving speed, depending on the configuration of the thrusters. The analytical expression of the function is (7):

$$F_z(V_z) = 28.528V_z^3 - 3.633V_z^2 + 44.425V_z \quad (7)$$

Using the characteristic curve of the thruster provided by the Blue Robotics manufacturer (Fig. 9), the propulsion speed of the ROV can be estimated in the main direction of travel (forward). This speed depends on the chosen configuration of the thrusters, because they are not symmetrical. The position of the thrusters that maximize the forward speed (Fig. 10). Considering this solution can calculate the thrust force

generated by the four identical thrusters mounted symmetrically with an angle of inclination of 45° with respect to the main moving direction.

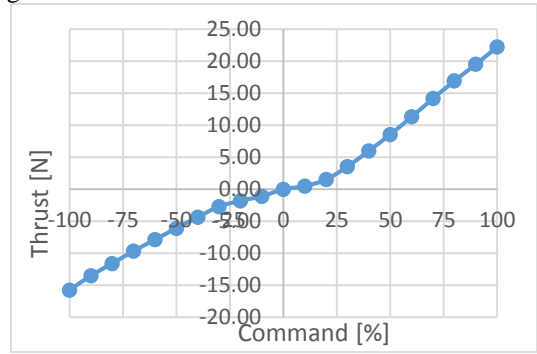


Fig.9. Propulsion Thrust [4]

For thruster's configuration (Fig.10) the pulling force generated by the four thrusters is achieved by projecting the force produced by each thruster on the movement direction.

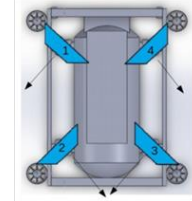


Fig.10. Thrusters position

Using the characteristic of the thrust shown in Fig.9, the maximum thrust force is $T_{max} = 22.25$ N.

$$F = 4 * \cos\left(\frac{\pi}{2}\right) * T_{max} \quad (8)$$

The force $F=63$ [N], the maximum speed of moving the ROV in the forward direction are $V_{zmax}=0.94$ [m/s].

CONCLUSION

This paper presents the underwater ROV system and simulation in Ansys Fluent. The results of simulate provide the data to design a housing ROV. The advantage of the simulated model is, it can be modified and optimized to achieve the expected performance with minimal effort.

The future simulation will analyses the accuracy of the data resulted. A set of experimental measurements will be performs to validate the model.

REFERENCE

- [1] Lazar I., Ghilezan A., Hnatiuc M., Development of Underwater Sensor Unit for Studying Marine Life, 2016 IEEE 22nd International Symposium for Design and Technology in Electronic Packaging (SIITME), Oradea, Romania, 2016, pp.82-86,
- [2] I. Masmitja, J Gonzalez, C Galarza, S Gomariz, J Aguzzi, et.all., New vectorial propulsion system and trajectory control designs for improved AUV mission autonomy, *Sensors*, 18(4), 1241, 2018
- [3] B. Allotta, R. Costanzib, L. P. A. Ridolfi, Identification of the main hydrodynamic parameters of Typhoon AUV from a reduced experimental dataset, *ELSEVIER*, Volume 147, 1 January 2018, Pages 77-88
- [4] <https://bluerobotics.com/software-and-hardware/>
- [5] E. M. Oantă, A.E. Dăscălescu, A. Sabău, Original Analytical Model of the Hydrodynamic Loads Applied on the Half-Bridge of a Circular Settling Tank, *ATOM-N 2016 Conference*, 25-28 August 2016, Constanta, Romania